ACS APPLIED MATERIALS & INTERFACES

Research Article

www.acsami.org

High-Performance, Room-Temperature, and No-Humidity-Impact Ammonia Sensor Based on Heterogeneous Nickel Oxide and Zinc Oxide Nanocrystals

Jian Wang,* Pan Yang, and Xiaowei Wei

School of Materials Science and Engineering, Xihua University, Chengdu 610039, P. R. China

Supporting Information

ABSTRACT: NiO nanocones decorated with ZnO nanothorns on NiO foil substrates are shown to be an ammonia sensor with excellent comprehensive performance, which could, in real-time, detect and monitor NH_3 in the surrounding environment. Gas-sensing measurements indicate that assembling nanocones decorated with nanothorns on NiO foil substrate is an effective strategy for simultaneously promoting the stability, reproducibility, and sensitivity of the sensor, because the NiO foil substrate as a whole can quickly and stably transfer electrons between the gas molecules and the sensing materials and the large specific surface area of both nanocones and nanothorns provide good accessibility of the gas molecules to the sensing materials. Moreover, p-type NiO, with majority charge carriers of holes, has higher binding affinity for the electron-donating ammonia, resulting in a significant increase in selectivity toward NH_3 over other organic gases. Compared with the NiO nanowires and pure NiO nanocones, the heterogeneous NiO nanocones/ZnO nanothorns exhibit less dependence on the temperature and humidity in response/recovery speed and sensitivity of sensing NH_3. Our investigation indicates that two factors are responsible for reducing the dependence on the gas sensing characteristics under various environmental conditions. One is that the n-type ZnO nanothorns growing on the surface of nanocones, with majority charge carriers of electrons, speed up adsorption and desorption of gas molecules. The other is that the abundant cone-shaped and thornlike superstructures on the substrate are favorable for constructing a hydrophobic surface, which prevents the gas sensing material from being wetted.

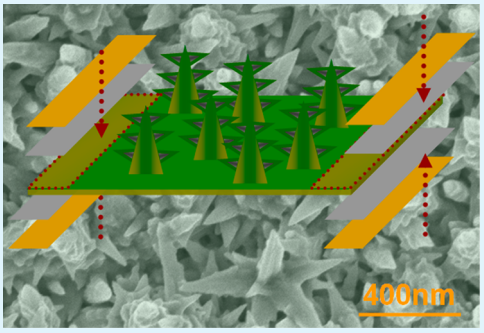

KEYWORDS: *nanocones, nanothorns, heteronanostructure, gas sensors, adsorption and desorption, gas sensing performance*

1. INTRODUCTION

Atmospheric environmental pollution has become one of the most serious issues that every country on earth is facing, which also has attracted considerable attention from a part of the scientific community to investigation of various environmental safety issues.[1−5] The major reason for atmospheric pollution is the release of harmful gases, liquids, and chemicals to the air through industrial effluents, agricultural chemicals, fertilizers, and so forth.[6,7] Ammonia (NH_3) is one of the toxic gases and is widely employed in refrigeration systems, livestock breeding, food processing, and fertilizer production.[8,9] Generally speaking, exposure at around 50 ppm of NH_3 gas in air may cause acute poisoning or life threatening situations, such as permanent blindness, lung disease, respiratory disease, skin disease, and so on.[7,10,11] Therefore, it became highly necessary to design and fabricate a long-term-reliable, highly-sensitive, miniaturized, room-temperature-efficient, and no-humidity-impact ammonia gas sensor, which can detect and monitor NH_3 concentration in real time in the surrounding environment. As a typical novel portable gas sensor with high performance, a chemical microgas sensor based on a semiconducting metal oxide is considered to be the leading candidate, which relies principally on continuously monitoring the direct changes of the conductance in adsorption and desorption of the target gas molecules.[12−14] Currently, some miniaturized chemical gas sensors based on nanoscale semiconductors have been successfully obtained and have excellent sensitivity due to their small size and the highly active surface of the gas sensing materials.[12,13,15] However, there are a number of obstacles that need to be overcome in order to further enhance gas sensitive performance and expand the range of application of such sensors: compatibility between stability and sensitivity, operability at room temperature, and the influence of humidity on the magnitude of the sensing signal.

Among these miniaturized gas sensing devices, the first type of gas sensor was based on NiO films or foils (i.e., two-dimensional nanomaterials), which owned significant repeatability and stability, but the sensitivity was usually very poor because of their small specific surface area.[16,17] The second type of gas sensor was based on NiO nanowires or nanotubes (i.e., one-dimensional nanomaterials), which had high sensitivity and fast response, however the stability was poor due to the poor

Received: December 16, 2014
Accepted: January 20, 2015
Published: January 20, 2015

DOI: 10.1021/am508807a
ACS Appl. Mater. Interfaces 2015, 7, 3816−3824

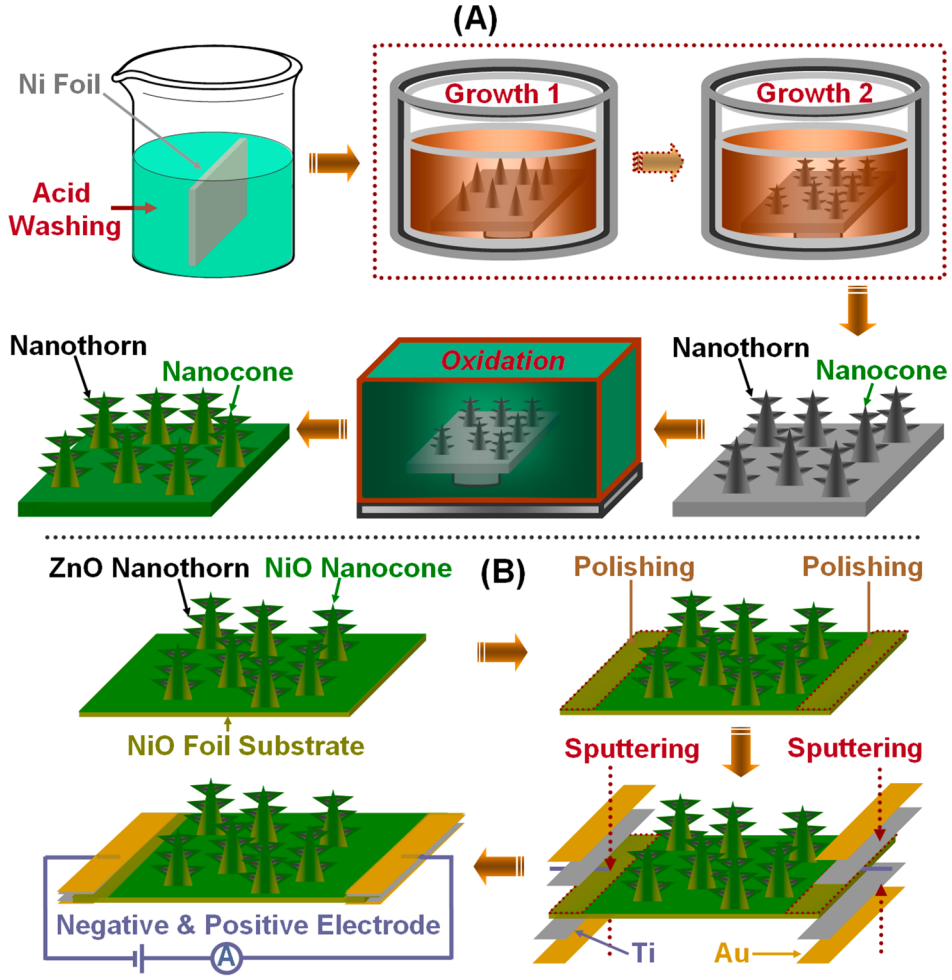

Figure 1. (A) Flowchart of samples fabrication shows the specific approach of synthesis of NiO nanocones decorated with ZnO nanothorns on NiO foil substrates. This unique conical structure was fabricated via a hydrothermal controllable reaction combined with a high temperature oxidation method. (B) Schematic diagram of the assembly processes and configuration of the gas sensing devices, which mainly contained the preparation of two electrodes and the connection between two edges of as-fabricated NiO foil and the electrodes.

interconnection between sensing materials and the electrodes.[18,19] In this work, our group combined NiO foils and NiO nanocones together to simultaneously promote the stability and sensitivity of the gas sensor. Furthermore, throughout the whole development history of oxide sensor, the majority of these gas sensing devices can carry out only at high temperature, not used in the existing environment of gas explosion.[20,21] The major issue is that the recovery performance of sensors is very poor at room temperature because the desorption of gas molecules adsorbed on the sensor takes a long time.[22,23] To solve this problem, we fabricated the nickel oxide nanocones decorated with zinc oxide nanothorns on nickel oxide foil substrates forming heterojunctions in the micro region, which greatly enhanced the response and recovery speed via improving electron transport and gas molecular diffusion in this special open nanostructure.

For commercial applications of gas sensing devices, one of the greatest obstacles is the influence of humidity on the magnitude of the gas sensor signal. This is because water vapor (i.e., humidity) is present in the real environment for detection or monitoring, and it strongly interacts with the surface or interface of a metal oxide semiconductor, which leads to a significant deterioration of the gas sensing properties.[24−26] Many strategies have been investigated to enhance response and recovery speed, for instance, extending the range of measurement parameters, increasing operation temperature, using hierarchical nanostructures, and introducing other species.[27−30] For our application, p−n heterojunction combining with special surface morphology would effectively exclude the cross-sensitivity between target gas and water vapor via unique a hydrophobic structure and enhance the response and recovery kinetics via high efficiency electron transfer. In the present work, we present a hydrothermal controllable route combined with high temperature oxidation approach to fabricate nickel oxide nanocones decorated with zinc oxide nanothorns on nickel oxide foil substrates and systematically investigate gas sensing properties of as-fabricated gas sensing devices. The results showed that the sensor owns excellent compatibility between stability and sensitivity, operability at room temperature, and reducing the impact of humidity for ammonia detection.

2. EXPERIMENTAL SECTION

2.1. Preparation of the Gas Sensing Materials. All the chemicals involved in this experiment were of analytical reagent (AR) grade (purity >99.0%) and were directly used without further purification. The specific strategies to fabricate the NiO nanocones decorated with ZnO nanothorns on NiO foil substrates were summarized as follows: (1) Ni foil was made via refining pure Ni

DOI: 10.1021/am508807a
ACS Appl. Mater. Interfaces 2015, 7, 3816−3824

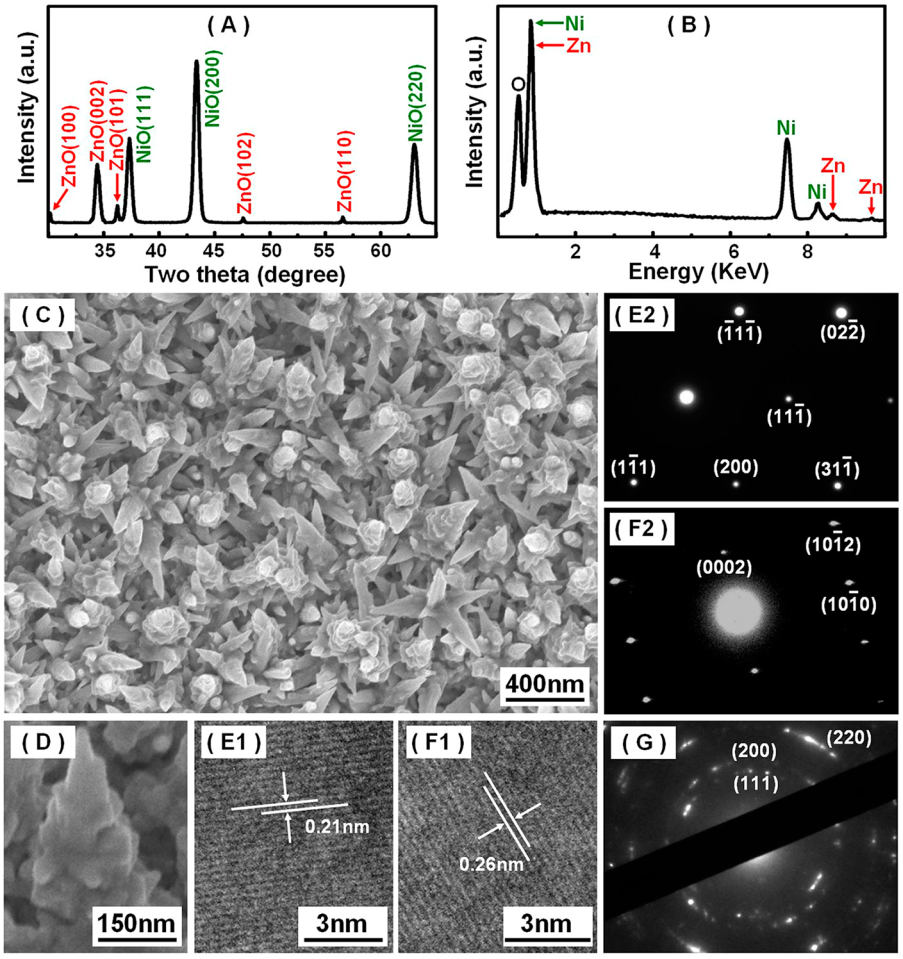

Figure 2. Structure and morphology characterization of the heterogeneous NiO nanocones/ZnO nanothorns on NiO foil substrates synthesized via the two-step hydrothermal reaction combined with subsequent high temperature oxidation method. (A) XRD pattern of the nanocones decorated with nanothorns confirming formation of cubic structure NiO. (B) EDS analysis confirming that the as-prepared products are composed of only Ni, Zn, and O elements. (C) SEM image of sample demonstrating nanocones distributing all over the NiO foil surface. (D) High-magnification SEM image of a single nanocone decorated with nanothorns. (E1, F1) HRTEM images recorded from the tops of both nanocone and nanothorn. (E2, F2) SAED patterns recorded from both a single nanocone and nanothorn, which show the single crystalline structure. (G) SAED pattern of substrate confirming that the NiO foil had a cubic structure and there is no other secondary phase.

(99.99%) in an arc furnace, followed via melt-plasma-spraying under nitrogen-protected atmosphere. As-prepared Ni foils were ultrasonically washed several times with ethanol, acetone, and distilled water for 30 min, respectively. Then as-treated Ni foils were dipped into the 18 wt % solution of sulfuric acid at 85 °C for 60 min to remove thin oxidation layer. (2) In a typical procedure of hydrothermal reaction, 0.476 g of nickel chloride hexahydrate ($NiCl_2{\cdot}6H_2O$) was dissolved into 30 mL distilled water under continuous magnetic stirring, and the color of the solution changed from colorless to homogeneous grass-green color within minutes, which demonstrated nickel ions were dispersed uniformly in the water solution. At this point, 30 mL distilled water solution of hydrazine hydrate ($N_2H_4{\cdot}H_2O$, 85 wt %) were dropwise added into the above solution. This reaction mixture was stirred constantly to obtain a homogeneous navy blue solution and subsequently was transferred into a Teflon-lined stainless steel autoclave containing as-treated Ni foil to perform hydrothermal reaction under a constant temperature for a definite time. (3) After the reaction was completed, step 2 was repeated for the as-fabricated Ni foil covering with gray−black products, and the $NiCl_2{\cdot}6H_2O$ was to be replaced with 0.273 g of zinc chloride ($ZnCl_2$). The resulting Ni foil was washed several times using ethanol and distilled water, respectively, and then, the products were dried in a vacuum oven at 100 °C for 10 h. (4) Following that, the as-fabricated foils were heated to 450 °C and kept at constant temperature for 8 h in a furnace in open air, and then, the furnace was cooled down to room temperature naturally. The resultant gray−green products on the foil substrate were collected for future characterization. Figure 1A shows the flowchart of fabrication of the NiO nanocones decorated with ZnO nanothorns on NiO foil substrates.

2.2. Assembling of the Gas Sensors. For the fabrication of the gas sensors (see Figure 1B), the as-prepared NiO nanocones decorated with ZnO nanothorns on NiO foil substrates used for the gas sensing materials. Specific procedure was as follows: (1) The edges of as-prepared NiO foil covering with NiO nanocones were polished using different specification sand paper; the as-polished two sides of NiO substrate were connected with the positive and negative electrodes using the homemade silver paste, respectively, and subsequently dried in the vacuum oven at 80 °C for 3 h. (2) In order to ensure the highest quality connection between substrate and electrodes, the junctions were strengthened via sputtering 20 nm pure titanium and 130 nm pure gold using a patterned mold in a magnetron sputtering apparatus. (3) The as-fabricated two electrodes were bound to the testing sockets using micrometer scale gold wires in a welding machine system. The resultant gas sensors were sonicated in ethanol and distilled washed and then blown dry with inert argon gas. Finally, heat treatment at 300 °C for 2 h in the vacuum oven was executed in order to optimize the contact between the gas sensing materials and the electrodes.

DOI: 10.1021/am508807a
ACS Appl. Mater. Interfaces 2015, 7, 3816−3824

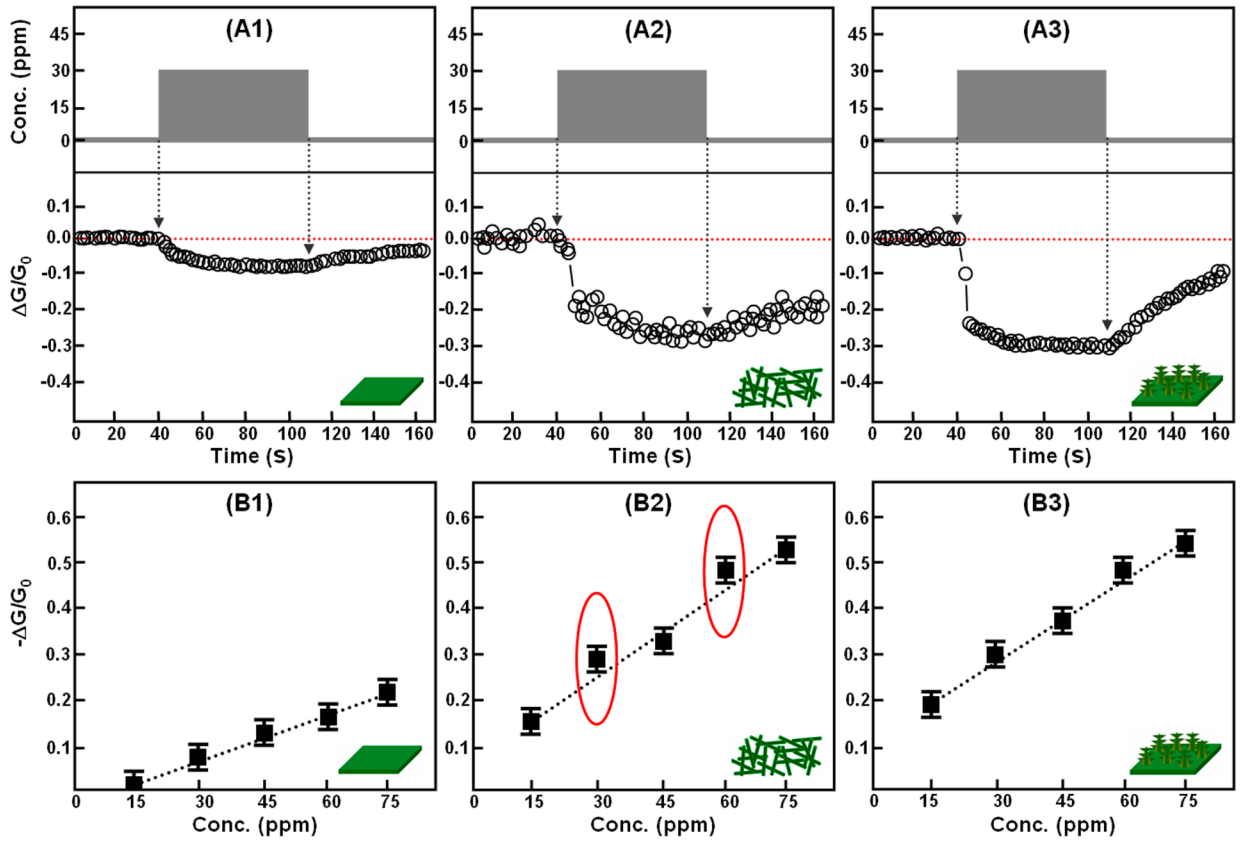

Figure 3. Stability and sensitivity test of sensors based on NiO gas sensing materials: conductance change of NiO foil, NiO nanowires, and NiO nanocones decorated with ZnO nanothorns on NiO foil substrates in dry atmosphere to 50 ppm (A1−A3) and different concentrations (B1−B3) of NH_3 at room temperature.

3. RESULTS AND DISCUSSION

3.1. Structure and Morphology of Gas Sensing Materials. Figure 2A shows the XRD patterns of the as-fabricated heterogeneous NiO nanocones/ZnO nanothorns on the foil. From the literature (Joint Committee on Powder Diffraction Standards (JCPDS) card No. 47-1049 and 36-1451), this mixed diffraction peaks were found to match with the mixed phases of both the face-centered cubic NiO phase and the hexagonal wurtzite ZnO phase, indicating that no other products existed in this heterogeneous nanocomposites. The texture coefficient of each crystal face of both nanocones and nanothorns can be calculated via the following formula:

$$TC_{hkl} = \frac{I_{(hkl)}/I_{0(hkl)}}{\sum I_{(hkl)}/I_{0(hkl)}} \times 100\% \quad (1)$$

where $I_{(hkl)}$ is the measured relative intensity of a place (hkl) and $I_{0(hkl)}$ is the standard intensity of the place (hkl) taken from the JCPDS data. The maximum texture coefficients of both NiO nanocones and ZnO nanothorns are $TC_{(200)\text{-NiO}}$ = 50% and $TC_{(002)\text{-ZnO}}$ = 60%, which indicates that the preferred orientations of both nanocones and nanothorns on different substrate are (200) and (002), respectively. Energy dispersive spectroscopy (EDS) analysis (Figure 2B) of the heterogeneous nanocomposites only revealed the peaks of Ni, Zn, and O, which further confirms that the as-synthesized NiO nanocones and ZnO nanothorns are high purity. Figure 2C presents the scanning electron microscopy (SEM) image of the NiO nanocones decorated with ZnO nanothorns distributing all over the NiO foil surface. The NiO nanocones have base diameters ranging from 100 to 300 nm and heights ranging from 150 to 400 nm; the diameters of ZnO nanothorns are about 30−50 nm and the heights can be up to 150 nm, which are consistent with the calculated values via Scherer's equation considering shape factor in our experiment.[31] More importantly, the heterogeneous yield is rather high and the branch is multitude as is evident from the NiO foil substrate. Figure 2D clearly demonstrates the morphology of a single nanocone. From this oblique view image it can be seen that the tip diameters of both nanocone and nanothorn are about 20 and 15 nm, respectively, and the apex angles of both nanocone and nanothorn are about 30°. In order to better understand the internal microstructure of the sharply pointed crystals in more detail, further high-resolution transmission electron microscopy (HRTEM) observation from the tops of both nanocone and nanothorn are shown in Figure 2E1 and F1, which show the crystal lattice structure. These clear lattice fringes indicate that the entire nanocone or nanothorn is single crystal structure, and no visible line or planar defects imply the high crystallinity of both NiO nanocone and ZnO nanothorns. These crystals are imaged to have nearly parallel lines, which are atomic planes separated via about 2.1 and 2.6 Å in Figure 2E1 and F1, corresponding to both the {200} planes of face-centered cubic NiO crystal and the {002} planes of hexagonal wurtzite ZnO crystal, respectively. Both the HRTEM images and SAED patterns demonstrate that the growth orientations of both NiO nanocone and ZnO nanothorn are along the [200] and [0002] directions, respectively, corroborated via above XRD results. The corresponding selected area electron diffraction (SAED) pattern of the heterogeneous nanocomposites is shown in

DOI: 10.1021/am508807a
ACS Appl. Mater. Interfaces 2015, 7, 3816−3824

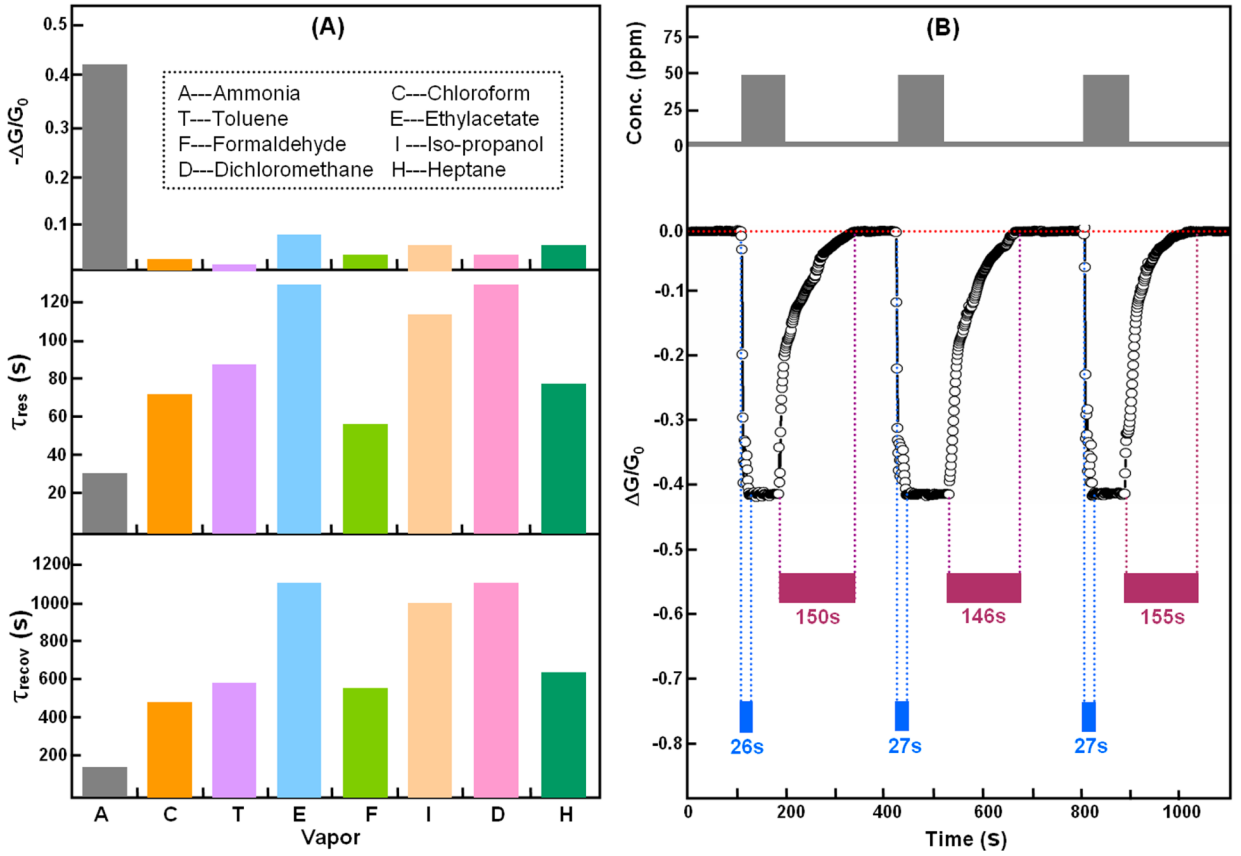

Figure 4. Selectivity and reproducibility test of the gas sensors based on NiO nanocones decorated with ZnO nanothorns. (A) Sensitivity (upper panel), response time (middle panel), and recovery time (bottom panel) of sensors in a dry atmosphere to different organic gases at room temperature. The concentration of NH_3 is 50 ppm, and the concentration of other organic gases is higher than 300 ppm. (B) Reproducibility of gas sensor in dry atmosphere to 50 ppm of NH_3 at room temperature.

Figure 2E2 and F2. These pattern spots also demonstrate the single crystal of both nanocone and nanothorn, and pattern spots can readily be indexed as (111), (200), and (220) of the face-centered cubic NiO and (100), (002), and (102) of the hexagonal wurtzite ZnO. The SAED pattern of NiO foil shown in Figure 2G, confirming that the NiO foil had a cubic structure, and there is no other secondary phase, which provides excellent growth substrate for nanocones decorated with nanothorns.

3.2. Stability and Sensitivity of the Gas Sensor. Figure 3A1−A3 shows the dynamic sensing transients of gas sensors based on NiO foil (Figure S1, Supporting Information), NiO nanowires (Figure S2, Supporting Information), and NiO nanocones decorated with ZnO nanothorns in a dry atmosphere to 30 ppm of NH_3 at room temperature. From the sensing transients, the NiO foil sensor has the shorter response time (20 s) and stable sensitive signals, because the bulk foil as a whole was able to quickly and stably transfer electrons between the gas molecules and the sensing materials. However, the gas sensitivity of this type of sensor is only about 10% (Figure 3A1). In contrast, the NiO nanowires sensor needs a longer response time (40 s) and its stability is poor (existing response errors); however, its sensitivity reaches up to 30% to 30 ppm of NH_3 (Figure 3A2), because the large specific surface area of NiO nanowires provided good accessibility of the gas molecules to the sensing materials.[32] These test results confirm the limitations of the pure components (such as a traditional bulk material or a nanomaterial) to act as ammonia sensors at room temperature. Therefore, our group combined the NiO foil and nanocones together to assemble the composite sensing materials, which simultaneously promotes the stability and sensitivity of sensor. As shown in Figure 3A3, when the sensor was exposed to 30 ppm of NH_3 in dry air, its conductance change displayed a significant decrease immediately with about 20 s. In contrast, when the flow of the NH_3 was switched off and that of air switched on, the conductance change recovered to its original value within about 90 s. Meanwhile, the sensor response and recovery were stable. The sensitivity and stability of the sensor were further examined upon consecutive exposure to different concentrations of NH_3 (Figure 3B1−B3) at room temperature. Linear behavior was observed for the sensitivity of the above three type sensors over the concentration range of 15−75 ppm for NH_3 in a dry atmosphere, which demonstrated the sensitivity increase with the increase of NH_3 concentration. Among them, the linear slope of sensitivity−concentration curves for sensors based on NiO nanowires and nanocones was found to be higher than that for the sensor on NiO foil. The sensitivity is related to the overall surface area of sensing materials and the concentration of gas molecules absorbed on the surface.[33] In addition, the sensitivity of the sensor based on NiO nanowires to 30 and 60 ppm was significantly higher than the linear value, which illustrated instability of sensitive signals. These results suggest that the assembling of NiO nanocones on NiO foil is an excellent strategy for simultaneously promoting the stability and sensitivity of the sensor.

DOI: 10.1021/am508807a
ACS Appl. Mater. Interfaces 2015, 7, 3816−3824

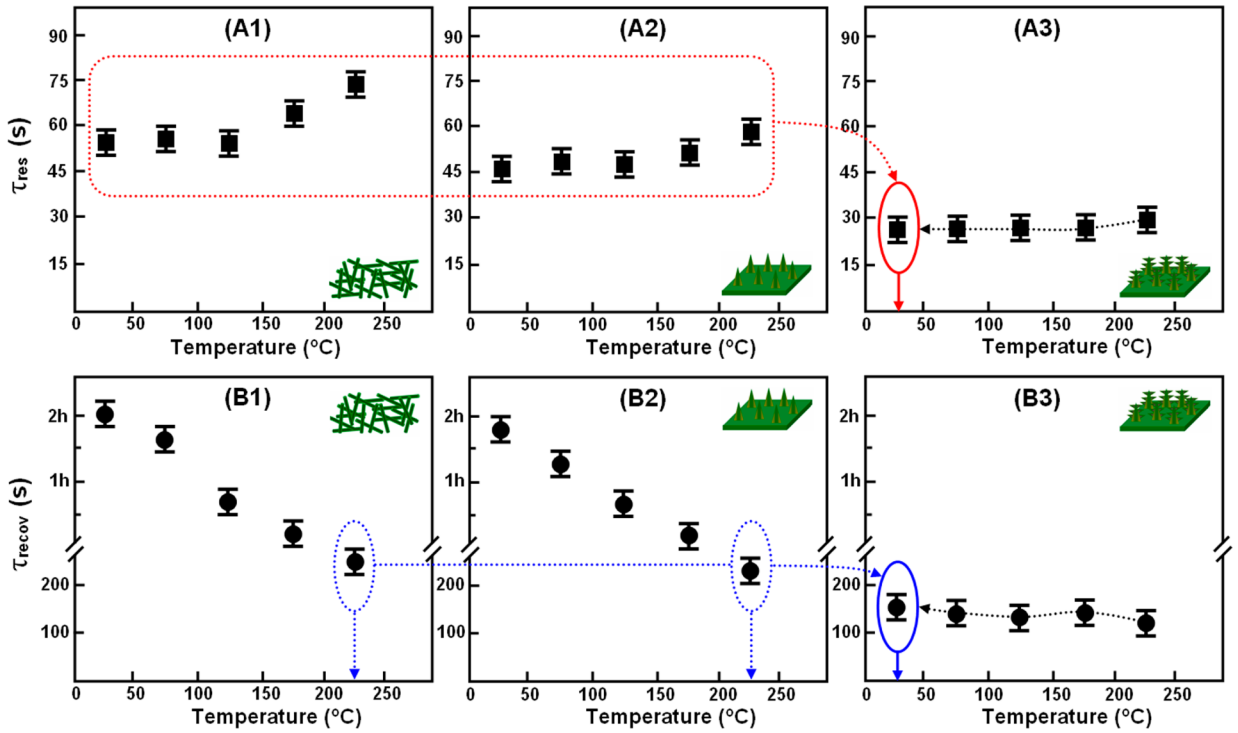

Figure 5. Operability of the gas sensor at room temperature. The response time (A1−A3) and recovery time (B1−B3) of gas sensors based on NiO nanowires, NiO nanocones on NiO foil substrates, and NiO nanocones decorated with ZnO nanothorns on NiO foil substrates in a dry atmosphere to 50 ppm of NH_3 at 25−225 °C. Compared with the NiO nanowires and nanocones, the heterogeneous nanocones/nanothorns exhibit less dependence on the working temperature in response/recovery speed, which could meet the requirements of routine testing.

3.3. Selectivity and Reproducibility of the Gas Sensor. Selectivity is one of the most important gas sensing properties of a sensor, which relies mainly on the specific interactions between the sensing materials and the target gas molecules. The gas sensing properties of a sensor based on NiO nanocones decorated with ZnO nanothorns toward a variety of toxic, corrosive, and flammable gases including ammonia, chloroform, toluene, ethyl acetate, formaldehyde, iso-propanol, dichloromethane, and heptane were explored to evaluate the selectivity of the sensor. The specific sensor parameters (sensitivity, response time, and recovery time) at room temperature are displayed in Figure 4A. Remarkably, the gas sensor based on nanocones decorated with nanothorns exhibited excellent selectivity to NH_3 when exposed to these interfering gases. For example, the sensitivity of sensors to 50 ppm of NH_3 was about 42%, whereas that sensitivity was less than 9% to a higher concentration (>300 ppm) of other gases. Furthermore, the response and recovery time to NH_3 are smaller than that of other organic gases. Several reasons might account for the excellent selectivity NH_3: first, every molecule of ammonia owns a lone electron pair and can readily donate the unpaired electrons (strong electron donating ability). The donating electrons could be transferred from the ammonia molecule to the gas sensing material, leading to a significant conductance change of the sensor.[34,35] Second, in a p-type semiconductor, holes are majority carriers. Therefore, p-type NiO nanocones might have higher binding affinity for the electron-donating ammonia. Last, the large active surface areas of the nanocones decorated with nanothorns available for direct sorption of ammonia molecules exist on the sensing materials; that is, selective physisorption to ammonia is also a key factor.[35]

Reproducibility is another key criterion for practical sensor applications, which is related with various factors including the connecting stability of sensing materials, contact stability between sensing materials and electrodes, and storage stability in air. Connecting and contact instability generally result in measurement error and can give fake response and recovery signals. Figure 3A3 and B3 clearly demonstrates that our sensor has excellent connection and contact stability. Therefore, we only tested the storage stability of the sensor in a dry atmosphere through repeatedly exposing it to 50 ppm of NH_3 at room temperature, as shown in Figure 4B. After storage in dry air for 10−20 days, the gas response of sensors was still maintained at about 42%, and the recovery abilities were not reduced after three sensing cycles (Figure 4B). More importantly, the response and recovery time were also kept at about 27 and 150 s, respectively, which indicated that the sensor based on NiO nanocones decorated with ZnO nanothorns has excellent reproducibility and reversibility under storage conditions.

3.4. Operability of the Gas Sensor at Room Temperature. As known, the common gas sensors are generally sensitive to working temperature. Therefore, we further investigated effects of operating temperature on sensor performances and expected that the sensor based on NiO nanocones decorated with ZnO nanothorns on NiO foils would show excellent gas sensing performance due to their p (NiO)−n (ZnO) heterojunction characteristics at room temperature. As shown in Figure 5A1 and A2, the response time of the sensors based on NiO nanowires (Figure S2, Supporting Information) and pure NiO nanocones (Figure S3, Supporting Information) gradually increases from 45 to 75 s to 50 ppm of NH_3 with increasing temperature (25−225 °C). In contrast, as shown in Figure 5B1 and B2, the recovery time of the corresponding two types of sensors linearly decreases from 2 h to 240 s with the increase of temperature (25−225 °C).

DOI: 10.1021/am508807a
ACS Appl. Mater. Interfaces 2015, 7, 3816−3824

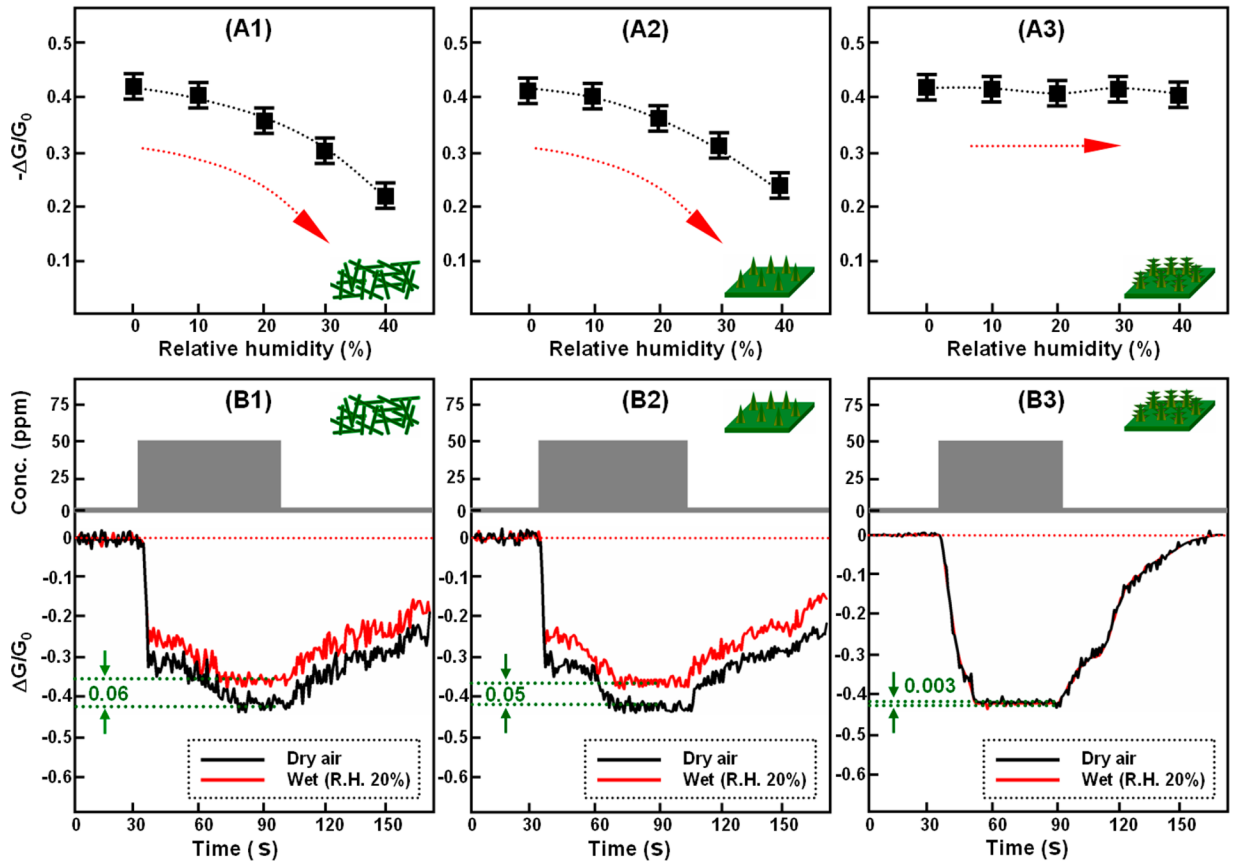

Figure 6. Influence of humidity on the gas sensing performance of sensors. (A1−A3) Sensitivity of gas sensors based on NiO nanowires, NiO nanocones on NiO foil substrates, and NiO nanocones decorated with ZnO nanothorns on NiO foil substrates in different relative humidity (R.H.) atmospheres to 50 ppm of NH_3 at room temperature. (B1−B3) Real-time response curves of different sensors in dry atmosphere and 20% R.H. to 50 ppm of NH_3 at room temperature.

This test result confirms that the operating temperature could influence gas sensing performance. However, in Figure 5A3 and B3, it can be found that the response and recovery time of sensor based on NiO nanocones decorated with ZnO nanothorns at higher temperatures than room temperature is still maintained at 27 and 150 s, respectively, which is consistent with test results at room temperature. Moreover, it should be noted that the sensor based on NiO nanocones decorated with ZnO nanothorns has shorter response and recovery times at room temperature, compared to sensors based on NiO nanowires or pure NiO nanocones. These results indicate that the response and recovery speeds of a sensor based on NiO nanocones decorated with ZnO nanothorns are almost not temperature dependent in our experiments; in other words, this sensor can work stably and effectively at room temperature, and no additional energy is need, which is very important for the practical applications of sensor. On the other hand, the above results also confirm that our p−n heterojunction-based sensors are workable in a temperature range of 25−225 °C, which could meet the requirements of routine testing.

High performance NH_3 sensing mechanism of (p-type) NiO nanocones decorated with (n-type) ZnO nanothorns on NiO foil substrates at room temperature involves adsorption and desorption of ammonia molecules on the metal oxide semiconductor surfaces and charge transfer between the surface of the sensing materials and the gas molecules, which leads to changes in its charge carrier concentrations and electrical conductivity.[36−39] When a p-type NiO semiconductor, with majority charge carriers of holes, is exposed to open air, the oxygen molecules adsorbed onto the NiO surface and chemisorption proceeded via the transfer of electrons from the surface to the oxygen molecules,[40] leading to increased carrier (hole) concentration near the surface and, consequently, decreased resistance. However, when this p-type NiO sensor is exposed to NH_3, the ammonia could catalytically react with the adsorbed oxygen via the transfer of electrons from the ammonia molecules to the NiO surface, leading to decreased carrier (hole) concentration near the surface, resulting in an increase in resistance of the sensing materials. In addition, if the electron density is high on the surface of gas sensing materials, the speed of adsorbed oxygen molecules becomes very fast. In NiO nanocones decorated with ZnO nanothorns, negative electrons of the n-type ZnO work as majority charge carriers, which can lead to quick adsorption of oxygen on the surface of nanothorns, thus speeding up the response speed of this sensor. It is well-known that the ammonia molecules can easily react with oxygen because the ammonia molecule owns a lone electron pair; that is, the recovery speed to NH_3 could be enhanced via assembling ZnO nanothorns on the surface of NiO nanocones.

3.5. Influence of Humidity on the Gas Sensing Performance. In order to investigate the influence of humidity on sensor signal, the sensitivity of gas sensors based on NiO nanowires (Figure S2, Supporting Information), NiO nanocones (Figure S3, Supporting Information), and NiO nano-

DOI: 10.1021/am508807a
ACS Appl. Mater. Interfaces 2015, 7, 3816−3824

cones decorated with ZnO nanothorns on NiO foil substrates were measured in different relative humidity (R.H.) atmospheres to 50 ppm of NH_3, as shown in Figure 6A1−A3. The sensitivity of nanowires sensor and pure nanocones sensor gradually decrease from quite a maximum value (42%) to a low value (23%) to 50 ppm of NH_3 with increasing relative humidity (0−40%). However, the sensitivity of sensor based on NiO nanocones decorated with ZnO nanothorns maintained at around 42% under the same conditions. This result indicates that the abundant cone-shaped and thorn-like superstructures on substrate are favorable for the constructing hydrophobic surface; available gas is trapped in spaces between the nanocones and nanothorns to form a gas-pocket at the rough surface water interface that prevents the gas sensing material from being wetted as much as possible.[41,42] To further uncover the extent of influence of humidity on the gas sensing performance, we investigated the dynamic sensing transients of the three type sensors in dry and 20% relative humidity atmospheres at room temperature (Figure 6B1−B3). Specifically, the sensitivity of the nanowires sensor and pure nanocones sensor to 50 ppm of NH_3 in dry atmosphere were all about 42%. In 20% R.H., the gas responses decreased by about 6% and 5%, respectively, compared with the sensitivity in dry atmosphere, which illustrates that the gas response of these two type sensors depends critically on the relative humidity. However, for the sensor based on NiO nanocones decorated with ZnO nanothorns, the sensitivity was not significantly changed at 42%, that is, the gas response became less dependent on the humidity. In practical applications, the highly reliable gas sensor with little or no dependence on humidity is extremely important, which will significantly increase the credibility and fidelity of sensitive signals and thus could open a new paradigm for the high performance gas sensor.

4. CONCLUSIONS

In summary, NiO nanocones decorated with ZnO nanothorns on NiO foil and their NH_3-sensing devices have been successfully fabricated. SEM observations reveal that the NiO nanocones have heights in the range 150−400 nm with base diameters varying from 100 to 300 nm and the ZnO nanothorns have heights of about 150 nm with base diameters varying from 30 to 50 nm. Combined XRD, EDS, HRTEM, and SAED demonstrate that the growth orientations of both NiO nanocone and ZnO nanothorn are along the [200] and [0002] directions, respectively. The gas sensing measurements show that the assembling NiO nanocones decorated with ZnO nanothorns on NiO foil substrate is an excellent strategy for simultaneously promoting the stability (almost no signal fluctuation) and sensitivity (reaches up to 30% to 30 ppm of NH_3) of sensor. Meanwhile, the gas response of this type of sensor is almost not temperature (the response and recovery times were maintained at 27 and 150 s to 50 ppm of NH_3 at different temperatures) and humidity (the sensitivity was maintained at around 42% to 50 ppm of NH_3 under the different humidity) dependent. In addition, we found that this sensor with unique gas-sensing materials also had excellent reproducibility and reversibility under storage conditions, fast response/recovery speed, high sensitivity, and good selectivity toward NH_3 over other organic gases.

The method of assembled nanocones decorated with nanothorns on foil substrate provides a significant impact for improvement and increased versatility in the fabrication of various structural and functional nanomaterials. Furthermore, the credibility, fidelity, and availability at different temperatures and humidities of gas sensing devices may pave an avenue toward low-cost, fast, and portable electronic noses for environmental monitoring.

■ ASSOCIATED CONTENT

Supporting Information

Morphology (SEM images) and structure (XRD patterns) characterization of NiO foil, NiO nanowires, and pure NiO nanocones. This material is available free of charge via the Internet at http://pubs.acs.org.

■ AUTHOR INFORMATION

Corresponding Author

*E-mail: wangjianxhu@163.com.

Notes

The authors declare no competing financial interest.

■ ACKNOWLEDGMENTS

We thank the Key Scientific Research Foundation of Xihua University (No. z1320110), Xihua University Young Scholars Training Program (No. 01201418), and the Open Research Subject of Key Laboratory (Research Base) of Special Materials Preparation and Control (Xihua University, No. szjj2014-059) for financial support.

■ REFERENCES

(1) Richards-Kortum, R.; Oden, M. Engineering. Devices for Low-Resource Health Care. *Science* **2013**, *342*, 1055−1057.

(2) Yang, H.; Flower, R. J.; Thompson, J. R. Pollution: China's New Leaders Offer Green Hope. *Nature* **2013**, *493*, 163.

(3) Henschler, D. Toxicological Problems Relating to Changes in the Environment. *Angew. Chem., Int. Ed.* **1973**, *12*, 274−282.

(4) Rumyantseva, M. N.; Gaskov, A. M.; Rosman, N.; Pagnier, T.; Morante, J. R. Raman Surface Vibration Modes in Nanocrystalline SnO_2 Prepared by Wet Chemical Methods: Correlations with the Gas Sensors Performances. *Chem. Mater.* **2005**, *17*, 893−901.

(5) Leclaire, J.; Husson, G.; Devaux, N.; Delorme, V.; Charles, L.; Ziarelli, F.; Desbois, P.; Chaumonnot, A.; Jacquin, M.; Fotiadu, F.; Buono, G. CO_2 Binding by Dynamic Combinatorial Chemistry: an Environmental Selection. *J. Am. Chem. Soc.* **2010**, *132*, 3582−3593.

(6) Wilkinson, K. E.; Palmberg, L.; Witasp, E.; Kupczyk, M.; Feliu, N.; Gerde, P.; Seisenbaeva, G. A.; Fadeel, B.; Dahlén, S.-E.; Kessler, V. G. Solution-Engineered Palladium Nanoparticles: Model for Health Effect Studies of Automotive Particulate Pollution. *ACS Nano* **2011**, *5*, 5312−5324.

(7) Timmer, B.; Olthuis, W.; van den Berg, A. Ammonia Sensors and Their Applications-a Review. *Sens. Actuators B* **2005**, *107*, 666−677.

(8) Narducci, D. Biosensing at the Nanoscale: There's Plenty of Room Inside. *Sci. Adv. Mater.* **2011**, *3*, 426−435.

(9) Bekyarova, E.; Kalinina, I.; Itkis, M. E.; Beer, L.; Cabrera, N.; Haddon, R. C. Mechanism of Ammonia Detection by Chemically Functionalized Single-Walled Carbon Nanotubes: in Situ Electrical and Optical Study of Gas Analyte Detection. *J. Am. Chem. Soc.* **2007**, *129*, 10700−10706.

(10) Sutti, A.; Baratto, C.; Calestani, G.; Dionigi, C.; Ferroni, M.; Faglia, G.; Sberveglieri, G. Inverse Opal Gas Sensors: Zn(II)-Doped Tin Dioxide Systems for Low Temperature Detection of Pollutant Gases. *Sens. Actuators B* **2008**, *130*, 567−573.

(11) Xu, X.; Fang, X.; Zeng, H.; Zhai, T.; Bando, Y.; Golberg, D. One-Dimensional Nanostructures in Porous Anodic Alumina Membranes. *Sci. Adv. Mater.* **2010**, *2*, 273−294.

(12) Wang, F.; Gu, H. W.; Swager, T. M. Carbon Nanotube/Polythiophene Chemiresistive Sensors for Chemical Warfare Agents. *J. Am. Chem. Soc.* **2008**, *130*, 5392−5393.

DOI: 10.1021/am508807a
ACS Appl. Mater. Interfaces 2015, 7, 3816−3824

(13) Wang, J.; Wei, L. M.; Zhang, L. Y.; Zhang, J.; Wei, H.; Jiang, C. H.; Zhang, Y. F. Zinc-Doped Nickel Oxide Dendritic Crystals with Fast Response and Self-Recovery for Ammonia Detection at Room Temperature. *J. Mater. Chem.* **2012**, *22*, 20038−20047.
(14) Wang, J.; Yang, F.; Wei, X.; Zhang, Y.; Wei, L.; Zhang, J.; Tang, Q.; Guo, B.; Xu, L. Controlled Growth of Conical Nickel Oxide Nanocrystals and Their High Performance Gas Sensing Devices for Ammonia Molecule Detection. *Phys. Chem. Chem. Phys.* **2014**, *16*, 16711−16718.
(15) Kumar, R.; Al-Dossary, O.; Kumar, G.; Umar, A. Zinc Oxide Nanostructures for NO2 Gas Sensor Applications: A Review. *Nano-Micro Lett.* **2014**, DOI: 10.1007/s40820-014-0023-3.
(16) Lee, C. Y.; Chiang, C. M.; Wang, Y. H.; Ma, R. H. A Self-Heating Gas Sensor with Integrated NiO Thin-Film for Formaldehyde Detection. *Sens. Actuators B* **2007**, *122*, 503−510.
(17) Sun, Q. Q.; Bao, S. J. Effects of Reaction Temperature on Microstructure and Advanced Pseudocapacitor Properties of NiO Prepared via Simple Precipitation Method. *Nano-Micro Lett.* **2013**, *5*, 289−295.
(18) Zhang, L.-S.; Jiang, L.-Y.; Chen, C.-Q.; Li, W.; Song, W.-G.; Guo, Y.-G. Programmed Fabrication of Metal Oxides Nanostructures Using Dual Templates to Spatially Disperse Metal Oxide Nanocrystals. *Chem. Mater.* **2010**, *22*, 414−419.
(19) Yang, Y.; Liu, L. F.; Güder, F.; Berger, A.; Scholz, R.; Albrecht, O.; Zacharias, M. Regulated Oxidation of Nickel in Multisegmented Nickel-Platinum Nanowires: an Entry to Wavy Nanopeapods. *Adv. Mater.* **2011**, *50*, 10855−10858.
(20) Epifani, M.; Diaz, R.; Arbiol, J.; Comini, E.; Sergent, N.; Pagnier, T.; Siciliano, P.; Taglia, G.; Morante, J. R. Nanocrystalline Metal Oxides From the Injection of Metal Oxide Sols in Coordinating Solutions: Synthesis, Characterization, Thermal Stabilization, Device Processing, and Gas-Sensing Properties. *Adv. Funct. Mater.* **2006**, *16*, 1488−1498.
(21) Rossinyol, E.; Prim, A.; Pellicer, E.; Arbiol, J.; Hernandez-Ramirez, F.; Peiro, F.; Cornet, A.; Morante, J. R.; Solovyov, L. A.; Tian, B. Z.; Bo, T.; Zhao, D. Y. Synthesis and Characterization of Chromium-Doped Mesoporous Tungsten Oxide for Gas Sensing Applications. *Adv. Funct. Mater.* **2007**, *17*, 1801−1806.
(22) Zhu, G. X.; Xu, H.; Liu, Y. J.; Xu, X.; Ji, Z. Y.; Shen, X. P.; Xu, Z. Enhanced Gas Sensing Performance of Co-Doped ZnO Hierarchical Microspheres to 1,2-Dichloroethane. *Sens. Actuators B* **2012**, *166*, 36−43.
(23) Russo, P. A.; Donato, N.; Leonardi, S. G.; Baek, S.; Conte, D. E.; Neri, G.; Pinna, N. Room-Temperature Hydrogen Sensing with Heteronanostructures Based on Reduced Graphene Oxide and Tin Oxide. *Angew. Chem., Int. Ed.* **2012**, *51*, 11053−11057.
(24) Chang, Y.-H.; Huang, Y.-T.; Lo, M. K.; Lin, C.-F.; Chenb, C.-M.; Feng, S.-P. Electrochemical Fabrication of Transparent Nickel Hydroxide Nanostructures with Tunable Superhydrophobicity/Superhydrophilicity for 2D Microchannels Application. *J. Mater. Chem. A* **2014**, *2*, 1985−1990.
(25) Li, Z. Y.; Zhang, H. N.; Zheng, W.; Wang, W.; Huang, H. M.; Wang, C.; MacDiarmid, A. G.; Wei, Y. Highly Sensitive and Stable Humidity Nanosensors Based on LiCl Doped TiO_2 Electrospun nanofibers. *J. Am. Chem. Soc.* **2008**, *130*, 5036−5037.
(26) Kim, H.-R.; Haensch, A.; Kim, II.-D.; Barsan, N.; Weimar, U.; Lee, J.-H. The Role of NiO Doping in Reducing the Impact of Humidity on the Performance of SnO_2-Based Gas Sensors: Synthesis Strategies, and Phenomenological and Spectroscopic Studies. *Adv. Funct. Mater.* **2011**, *21*, 4456−4463.
(27) Joo, S.; Muto, I.; Hara, N. Hydrogen Gas Sensor Using Pt- and Pd-Added Anodic TiO_2 Nanotube Films. *J. Electrochem. Soc.* **2010**, *157*, J221−J226.
(28) Yang, D.-J.; Kamienchick, I.; Youn, D. Y.; Rothchild, A.; Kim, I.-D. Ultrasensitive and Highly Selective Gas Sensors Based on Electrospun SnO_2 Nanofibers Modified by Pd Loading. *Adv. Funct. Mater.* **2010**, *20*, 4258−4264.
(29) Choi, J.-K.; Hwang, I.-S.; Kim, S.-J.; Park, J.-S.; Park, S.-S.; Jeong, U.; Kang, Y.-C.; Lee, J.-H. Design of Selective Gas Sensors Using Electrospun Pd-Doped SnO_2 Hollow Nanofibers. *Sens. Actuators B* **2010**, *150*, 191−199.
(30) Willett, K. M.; Gillett, N. P.; Jones, P. D.; Thorne, P. W. Attribution of Observed Surface Humidity Changes to Human Influence. *Nature* **2007**, *446*, 710−712.
(31) Pathak, D.; Bedi, R. K.; Kaur, D. Growth of Heteroepitaxial $AgInSe_2$ Layers on Si (100) Substrates by Hot Wall Method. *Optoelectron. Adv. Mater.* **2010**, *4*, 657−661.
(32) Franke, M. E.; Koplin, T. J.; Simon, U. Metal and Metal Oxide Nanoparticles in Chemiresistors: Does the Nanoscale Matter? *Small* **2006**, *2*, 36−50.
(33) Kauffman, D. R.; Star, A. Carbon Nanotube Gas and Vapor Sensors. *Angew. Chem., Int. Ed.* **2008**, *47*, 6550−6570.
(34) Hagfeldt, A.; Gratzel, M. Light-Induced Redox Reactions in Nanocrystalline Systems. *Chem. Rev.* **1995**, *95*, 49−68.
(35) Virji, S.; Huang, J.; Kaner, R. B.; Weiller, B. H. Polyaniline Nanofiber Gas Sensors: Examination of Response Mechanisms. *Nano Lett.* **2004**, *4*, 491−496.
(36) Ding, M. N.; Star, A. Selecting Fruits with Carbon Nanotube Sensors. *Angew. Chem., Int. Ed.* **2012**, *51*, 7637−7638.
(37) King, B. H.; Gramada, A.; Link, J. R.; Sailor, M. J. Internally Referenced Ammonia Sensor Based on an Electrochemically Prepared Porous SiO_2 Photonic Crystal. *Adv. Mater.* **2007**, *19*, 4044−4048.
(38) Lu, G.; Ocola, L. E.; Chen, J. Room-Temperature Gas Sensing Based on Electron Transfer between Discrete Tin Oxide Nanocrystals and Multiwalled Carbon Nanotubes. *Adv. Mater.* **2009**, *21*, 2487−2491.
(39) Li, L.; Gao, P.; Baumgarten, M.; Müllen, K.; Lu, N.; Fuchs, H.; Chi, L. High Performance Field-Effect Ammonia Sensors Based on a Structured Ultrathin Organic Semiconductor Film. *Adv. Mater.* **2013**, *25*, 3419−3425.
(40) Volanti, D. P.; Felix, A. A.; Orlandi, M. O.; Whitfield, G.; Yang, D.-J.; Longo, E.; Tuller, H. L.; Varela, J. A. The Role of Hierarchical Morphologies in the Superior Gas Sensing Performance of CuO-Based Chemiresistors. *Adv. Funct. Mater.* **2013**, *23*, 1759−1766.
(41) Lai, Y.; Gao, X.; Zhuang, H.; Huang, J.; Lin, C.; Jiang, L. Designing Superhydrophobic Porous Nanostructures with Tunable Water Adhesion. *Adv. Mater.* **2009**, *21*, 3799−3803.
(42) Maitra, T.; Tiwari, M. K.; Antonini, C.; Schoch, P.; Jung, S.; Eberle, P.; Poulikakos, D. On the Nanoengineering of Superhydrophobic and Impalement Resistant Surface Textures below the Freezing Temperature. *Nano Lett.* **2014**, *14*, 172−182.

DOI: 10.1021/am508807a
ACS Appl. Mater. Interfaces 2015, 7, 3816−3824